BJD
British Journal of Dermatology

Imaging of basal cell carcinoma by high-definition optical coherence tomography: histomorphological correlation. A pilot study

M.A.L.M. Boone,[1] S. Norrenberg,[1] G.B.E. Jemec[2] and V. Del Marmol[1]

[1]Department of Dermatology, Hôpital Erasme, Université Libre de Bruxelles, 1070 Brussels, Belgium
[2]Department of Dermatology, Roskilde Hospital, Health Sciences Faculty, University of Copenhagen, Denmark

Correspondence
Marc Boone.
E-mail: dr.boone@scarlet.be

Accepted for publication
30 June 2012

Funding sources
None.

Conflicts of interest
None declared.

DOI 10.1111/j.1365-2133.2012.11194.x

Summary

Background With the continued development of noninvasive therapies for basal cell carcinoma (BCC) such as photodynamic therapy and immune therapies, noninvasive diagnosis and monitoring become increasingly relevant. High-definition optical coherence tomography (HD-OCT) is a high-resolution imaging tool, with micrometre resolution in both transversal and axial directions, enabling visualization of individual cells up to a depth of around 570 μm, and filling the imaging gap between conventional optical coherence tomography (OCT) and reflectance confocal microscopy (RCM).

Objectives We sought to determine the feasibility of detecting BCC by this technique using criteria defined for RCM and conventional OCT and compared with histology.

Methods In this pilot study skin lesions of 21 patients with a histologically proven BCC were imaged by HD-OCT just before excision and images analysed qualitatively.

Results Features for four different BCC subtypes were described in both transverse and axial directions. In general, these features were subepidermal or intradermal aggregations of cells. These islands or trabeculae were surrounded by a less refractile border corresponding with palisading and peritumoral mucin production. There was a pronounced architectural disarray of the epidermis. A variably refractile stroma together with abundant dilated peritumoral blood vessels was present. These features were comparable with histological features for each patient.

Conclusions Using features already suggested by RCM and conventional OCT, the study implies that HD-OCT facilitates *in vivo* diagnosis of BCC and allows the distinction between different BCC subtypes for increased clinical utility.

Basal cell carcinoma (BCC) continues to be the most common cancer occurring in humans worldwide and is becoming a major public health problem.[1,2] It is a multifactorial disease although most lesions are related to excess sun exposure.[3,4] Clinical–pathological correlation is essential when planning the treatment of a BCC.[5] Different noninvasive imaging techniques have proved successful in facilitating diagnosis of BCC.[6–14]

We have recently introduced high-definition optical coherence tomography (HD-OCT). This is an innovative technique based on the principle of conventional optical coherence tomography (OCT), with the ability to carry out optical imaging up to 570 μm deep within highly scattering media such as skin and with a micrometre resolution in both lateral and axial directions, giving it the potential to visualize individual cells.[15] HD-OCT therefore provides morphological imaging which permits visualization of individual cells to a considerably greater depth than reflectance confocal microscopy (RCM), which has hitherto been the only technology offering imaging of individual cells *in vivo*. Additionally, HD-OCT also provides cross-sectional imaging like the conventional OCT, potentially giving the method considerable diagnostic utility.

RCM has been used to describe histopathological features of BCC *in vivo*, with the confocal features shown to have good histological correlation.[12–14] Similarly, diagnostic criteria for BCC in conventional OCT have been suggested.[6]

The aim of this pilot study is to compare RCM and conventional OCT imaging criteria with HD-OCT images and on the basis of this to suggest relevant HD-OCT imaging criteria for the *in vivo* diagnosis of BCC and for the differentiation of BCC subtypes compared with histology.

Materials and methods

Patients

Twenty-one fair-skinned patients (Fitzpatrick types II and III) with a single histologically proven BCC lesion each located on the face, arms, legs or trunk were recruited for this pilot study. Signed informed consent was obtained. The group included 11 women and 10 men with ages ranging from 41 to 87 years. Histopathological examination of the 21 biopsy specimens revealed features diagnostic of nodular BCC in five cases, infundibulocystic BCC in two cases, superficial BCC in six cases and infiltrative BCC in eight cases. HD-OCT was performed on these lesions just before excision (Table 1).

High-definition optical coherence tomography

HD-OCT is based on the principle of conventional OCT, specifically the ability to carry out optical imaging deep within highly scattering media such as skin, with micrometre resolution in both transverse and axial directions, in order to visualize individual cells (Skintell®; Agfa Healthcare, Mortsel, Belgium). Instead of a single pin diode, it uses a two-dimensional, infrared-sensitive (1000–1700 nm) imaging array for light detection. This enables focus tracking: the focal plane is continuously moved through the sample. The movements of the focal plane and the reference mirror are synchronized, and the refractive index of the sample is taken into account. This results in a high lateral resolution of 3 μm at all depths of the sample. A high axial resolution (3 μm in skin) is achieved using a broadband thermal light source combined with a special filter. This technology offers high resolution in all three dimensions. Moreover, the system is capable of capturing a slice image and an *en face* image in real time, as well as fast three-dimensional acquisition. The spectral sensitivity makes it possible to work in the near infrared range above 1000 nm. The field of view is 1·8 × 1·5 mm. The tissue penetration depth is up to 570 μm, and the total light power at the tissue is less than 3·5 mW. The system works in direct contact with the skin, using an optical matching gel (Skintell® optical gel; Agfa Healthcare) comparable with ultrasound gel. The interference signal detected by the two-dimensional imaging sensor is digitized, and its envelope of the interference signal is calculated (extraction of reflection strength from the interference signal). The result is transferred to a computer and displayed using a greyscale or colour palette, thereby generating an OCT image. Further technical details are discussed elsewhere.[15]

Diagnostic criteria for basal cell carcinoma

The histological features of BCC on formalin-fixed, paraffin-embedded tissues include parakeratosis; actinic changes in the overlying epidermis; islands of basaloid cells with monomorphic hyperchromatic nuclei and scant poorly demarcated cytoplasm; mitotic figures; apoptotic cells; and palisading of the basaloid cells at the periphery of the islands. These islands of tumour cells are surrounded by an abundant mucinous stroma with separation of the tumour cells from the surrounding stroma (clefting). Prominent increased vascularity is also noted, as well as solar elastosis and variable amounts of predominantly mononuclear inflammatory cells with scattered neutrophils.[16]

A set of five confocal imaging criteria was formulated by analysing biopsy-correlated confocal images.[12] These criteria are: presence of elongated monomorphic basaloid nuclei; polarization of these nuclei along the same axis of orientation; prominent inflammatory infiltrate; increased vasculature; and pleomorphism of the overlying epidermis indicative of actinic damage.

Similarly, in conventional OCT four common features of BCC tumour tissue were observed: dark lobular structures and pattern of abnormal architecture; at the periphery of the lobules decreased reflectance appearing darker than the bulk of the lobules; highly reflective margins surrounding the lobules corresponding with fibrous stroma; and dilated blood vessels.[6]

Data analysis

This entailed implementation of the five RCM imaging criteria of BCC on the *en face* HD-OCT images and of the four conven-

Table 1 Tumour and patient characteristics per histological subtype of basal cell carcinoma (BCC)

Histological subtype	Nodular BCC	Infundibulocystic BCC	Superficial BCC	Infiltrative BCC
Number of patients	5	2	6	8
Number of tumours	5	2	6	8
Mean patient age (years)	68	71	65	62
Gender (F/M)	2/3	1/1	3/3	5/3
Tumour localization				
Head/neck	3	2	0	3
Trunk	2	0	6	4
Arms	0	0	0	0
Legs	0	0	0	1

tional OCT features of BCC on the cross-sectional HD-OCT images. Haematoxylin and eosin (H&E)-stained histological vertical sections of these 21 lesions were correlated with the corresponding HD-OCT images in order to identify relevant HD-OCT imaging criteria for the *in vivo* diagnosis of BCC and for the differentiation of BCC subtypes.

Results

Histopathological features

All 21 biopsy specimens were examined. All these specimens exhibited characteristic histopathological features of BCC with four morphological subtypes, five nodular, two infundibulocystic, six superficial and eight infiltrative BCC.

The histological features on formalin-fixed, paraffin-embedded tissues of nodular BCC include actinic changes in the overlying epidermis; islands of basaloid cells with monomorphic hyperchromatic nuclei and scant poorly demarcated cytoplasm; mitotic figures; apoptotic cells; and palisading of the basaloid cells at the periphery of the islands. These islands of tumour cells were surrounded by an abundant mucinous stroma with separation of the tumour cells from the surrounding stroma (clefting). Prominent increased vascularity was also noted with variable amounts of predominantly mononuclear cells. Solar elastosis was observed (Fig. 1a). The infundibulocystic BCCs presented keratin-filled cysts. Reticulated basaloid cells with some mitotic activity and mucin production were observed. The stromal reaction was minimal (Fig. 2a). In the superficial BCCs the small, discrete islands of basaloid cells presented intermittently along the basal layer. All islands were in contact with the epidermis. There was a prominent peripheral palisading and peritumoral mucin production. The stromal reaction was prominent (Fig. 3a). The infiltrating forms presented elongated islands and cords of atypical basal cells widely separated spatially. The nests of tumour cells were often angulated and oriented almost perpendicular to the surface. Palisading was not as well developed. The stroma was minimal and more fibrotic (Fig. 4a). Table 2 summarizes these histopathological features.

High-definition optical coherence tomography

When imaging the nodular BCC in real time, cross-sectional mode lobular patterns of abnormal architecture can be perceived together with dilated blood vessels and highly reflective margins (Fig. 1b). In *en face* imaging the nodular BCC islands of tumour cells were noted associated with intervening areas of low reflectivity which may correspond to a mucinous stroma surrounding a rim of low-reflective tumour cells (palisading). Inside this low-reflective zone tumour cells are much more reflective. Abundant blood vessels were seen juxtaposed to BCC cells. It is not possible to visualize rolling of leucocytes as in RCM. There is a variable reflective stroma with

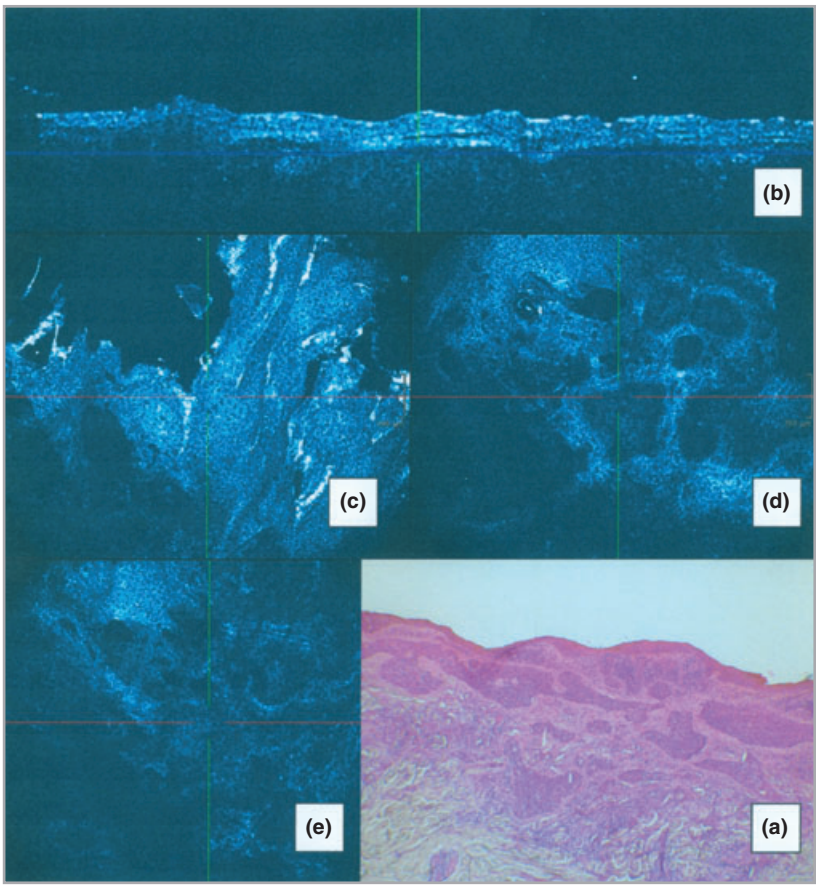

Fig 1. Nodular basal cell carcinoma (BCC). (a) Haematoxylin and eosin-stained histological section shows actinic changes in overlying epidermis, islands of basaloid cells with palisading. These islands are surrounded by an abundant mucinous stroma with separation of the tumour cells from the surrounding stroma (clefting). Prominent peritumoral stromal reaction. (b) In high-definition optical coherence tomography (HD-OCT) slice mode lobular patterns of abnormal architecture are perceived with dilated blood vessels and high-reflective margins. (c) In HD-OCT *en face* mode the overlying epidermis presents an architectural disarray with parakeratosis, pleomorphism and some degree of keratinocyte atypia with variably sized nuclei at the basal cell layer. (d) In *en face* HD-OCT imaging the nodular BCC islands of tumour cells are noted with intervening areas of low refractility. Inside this low-refractile zone tumour cells are more refractile. Abundant blood vessels are seen juxtaposed to the islands. (e) *En face* HD-OCT imaging shows a variable refractile stroma with inflammatory cells.

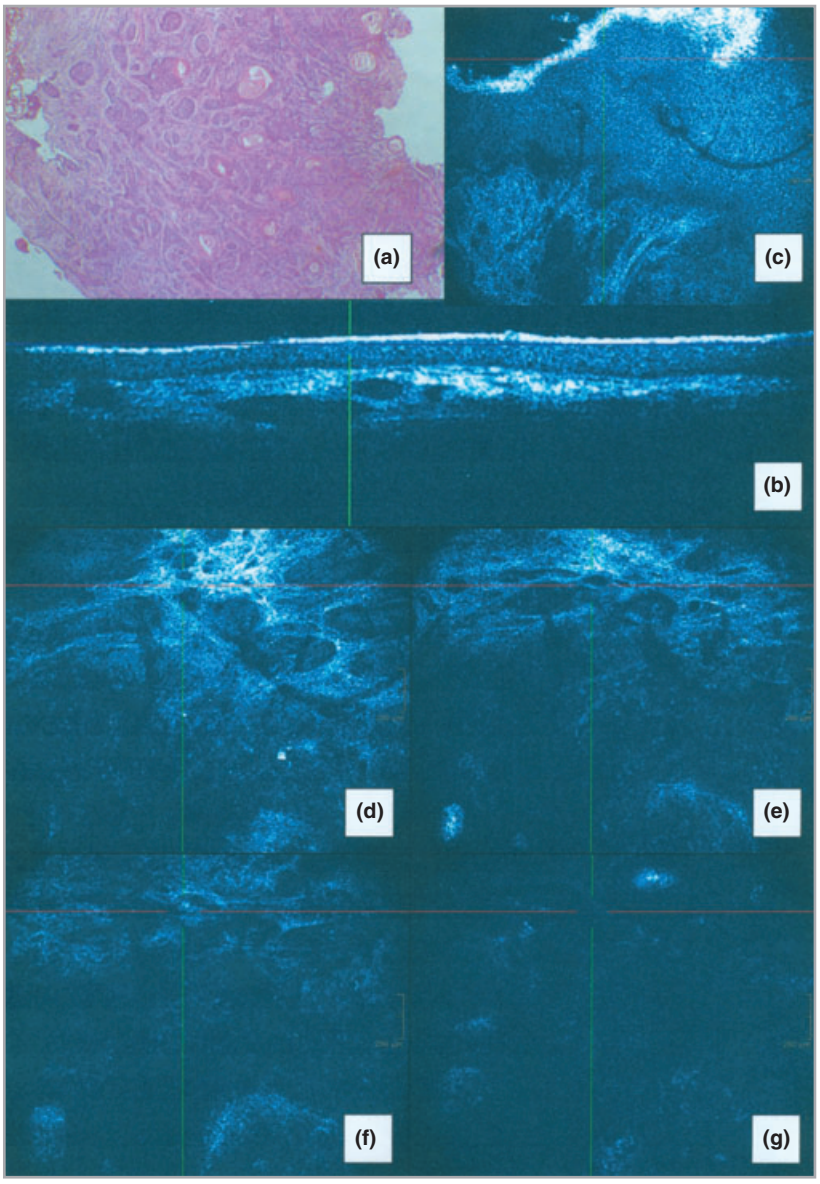

Fig 2. Infundibulocystic basal cell carcinoma. (a) Haematoxylin and eosin-stained histological section presents keratin-filled cysts. Reticulated basaloid cells and mucin production are observed. The stromal reaction is minimal. (b) Slice high-definition optical coherence tomography (HD-OCT) imaging shows multiple low-refractile cystic lesions. Solar elastosis is present. (c) *En face* HD-OCT imaging of the epidermis shows architectural disarray. (d–g) *En face* HD-OCT imaging from papillary dermis to reticular dermis displays multiple cystic lesions sometimes filled with highly refractile particles. The stromal reaction is present.

inflammatory cells intermixed. The overlying epidermis presented an architectural disarray with parakeratosis, pleomorphism and some degree of keratinocyte atypia with variably sized nuclei at the basal cell layer. The BCC cells appeared to be elongated with their nuclei oriented along the same principal axis, thus manifesting a polarized appearance. These tumour cells were monomorphic in shape with a high nuclear/cytoplasmic ratio: nuclei appearing dark (low contrast) whereas the cytoplasm appeared bright. Nucleoli could not be observed. On the contrary, solar elastosis was evident in several specimens (Fig. 1c–e).

Imaging of infundibulocystic BCC demonstrated several low-reflective cystic lesions sometimes filled with highly reflective particles. Epidermal disarray is present. The stromal reaction is minimal (Fig. 2b–g).

On imaging in slice mode of the superficial BCC, immediately subepidermal aggregates of tumour cells were observed. There was a peritumoral weakly reflective zone (Fig. 3b). *En face* imaging showed inflammatory cells scattered in the peritumoral stroma. Abundant dilated peritumoral blood vessels were perceived. Solar elastosis was obvious in some species. Deeper in the papillary dermis and upper dermis highly reflective margins surrounding the lobules and corresponding with fibrous stroma were observed (Fig. 3c–g).

On imaging of infiltrative BCC (Fig. 4b–g), lobular patterns of abnormal architecture can be perceived together with dilated blood vessels and highly reflective margins. Elongated low-reflective islands and cords were noticed in *en face* mode. The architectural disarray of the epidermis and solar elastosis were evident. At the level of the papillary dermis and upper reticular dermis low-reflective tumoral aggregates are surrounded by highly reflective margins corresponding with fibrous stroma. Scattered mildly reflective inflammatory cells were observed (Table 2).

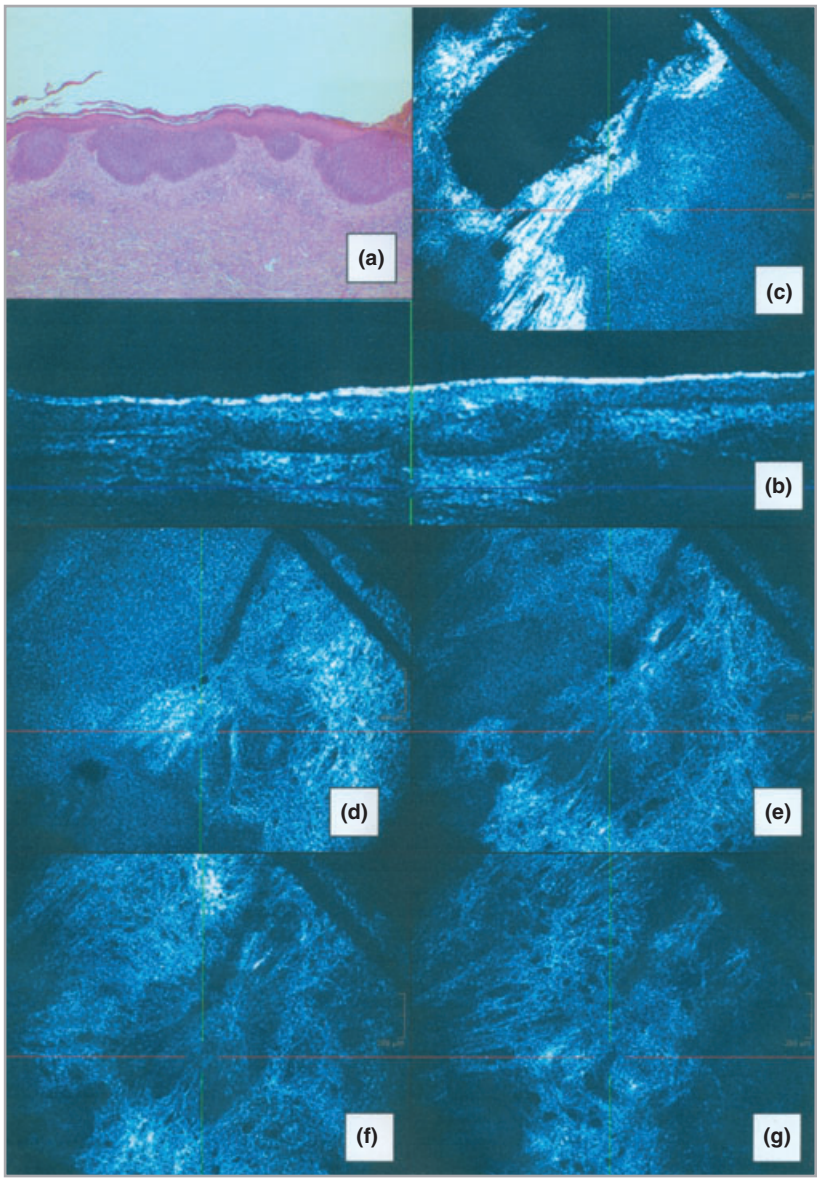

Fig 3. Superficial basal cell carcinoma. (a) Haematoxylin and eosin-stained histological section shows discrete islands of basaloid cells presented intermittently along the basal layer. Peripheral palisading is prominent as well as the stromal reaction. (b) In high-definition optical coherence tomography (HD-OCT) slice mode an subepidermal aggregate is demonstrated. There is a peritumoral weakly refractile zone. (c) In HD-OCT *en face* mode an epidermal architectural disarray is observed. (d–g) In HD-OCT *en face* mode in papillary dermis and upper dermis highly reflective margins surrounding the lobules corresponding with fibrous stroma are presented. Inflammatory cells scattered in the peritumoral stroma are demonstrated.

The imaging features of BCC by RCM and by multibeam OCT (MB-OCT) as described in the literature are displayed in Table 3. These features were implemented on HD-OCT images.

Discussion

We have explored the capability of HD-OCT to detect BCC. Features defined for RCM and conventional OCT were compared with histology. Features of BCC detected by both techniques can be observed by HD-OCT (Table 3), suggesting that HD-OCT fills the imaging gap between RCM and conventional OCT. Comparison between the different noninvasive imaging methods (RCM, HD-OCT, MB-OCT) in a head-to-head manner of the lesions *in vivo* was not done due to organizational difficulties and the need first to establish HD-OCT vis-à-vis the gold standard of histology.

The data suggest that subclassification of BCC is possible *in vivo*. HD-OCT features of BCCs of four different subtypes were described in both transverse and axial directions (Table 2). BCCs have traditionally been classified histologically according to their degree and mode of differentiation. However, there is an accumulating body of evidence suggesting that the growth pattern of the neoplasm is more relevant than the degree of differentiation from the perspective of providing the clinician with information that may be helpful in planning the optimal therapeutic procedure.[17] According to Rigel's classification of BCCs,[17] the circumscribed BCC group encompasses other types besides the typical and most common nodular BCC. Infundibulocystic BCC or follicular BCC is a peculiar variant of the circumscribed BCC group that occurs on the face. The observed HD-OCT features of infundibulocystic BCC seems to be quite different compared with nodular BCC. Therefore the aim of this paper is not only to

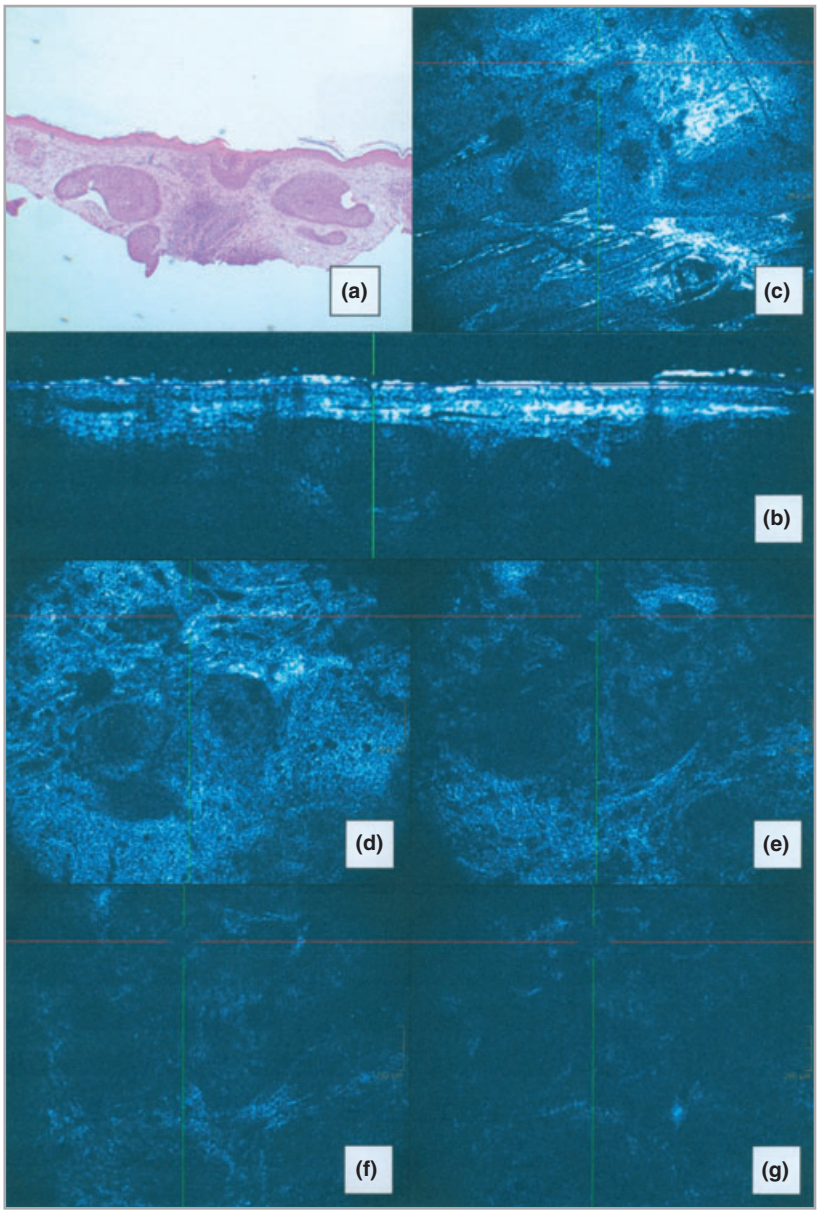

Fig 4. Infiltrative basal cell carcinoma. (a) Haematoxylin and eosin-stained histological section shows elongated islands of atypical basal cells widely separated spatially. The stroma is more fibrotic. (b) In high-definition optical coherence tomography (HD-OCT) slice mode lobular patterns of abnormal architecture are perceived together with dilated blood vessels and highly reflective margins. (c) The architectural disarray of the epidermis and solar elastosis is evident in the HD-OCT *en face* mode. (d–g) In *en face* HD-OCT imaging from papillary dermis to reticular dermis low-refractile tumoral aggregates are surrounded by highly reflective margins corresponding with fibrous stroma. Scattered mildly refractile inflammatory cells are observed.

focus on what is similar in all BCC lesions but also on more distinguishing features.

The vocabulary used to describe the characteristic features of BCC in conventional OCT and RCM was adopted in this study in order to provide a terminological continuum. In general these features were high subepidermal or intradermal aggregations of cells. These lobulated nodules, islands or trabeculae were surrounded by a less-reflective border possibly corresponding with palisading and/or peritumoral mucin production. Within these tumour aggregates brightly reflective cells and structures were demonstrated. There was a pronounced architectural disarray of the epidermis. A variably reflective stroma with inflammatory cells together with abundant dilated peritumoral blood vessels was present. Solar elastosis was obvious in several biopsies. Deeper in the papillary dermis and upper reticular dermis highly reflective margins surrounding the lobules corresponding with fibrous stroma were observed in cross-sectional images. A distortion ('streaming effect') of the collagen network probably provoked by the pressure of the tumour islands was observed in *en-face* images. To the best of our knowledge, this particular feature has never been described before.

We found that these features generally correlated very well with the H&E-stained biopsy sections (Table 2). Features that were readily identified by both HD-OCT and standard microscopy of H&E-stained sections included parakeratosis, actinic changes overlying the BCC, relative monomorphism of BCC cells, BCC nuclei exhibiting elongated or oval appearance, high nuclear/cytoplasmic ratios, mucin deposition, increased vascularity and prominent inflammatory cell infiltrate and solar elastosis. Uniform polarization of BCC nuclei observed by HD-OCT and the highly reflective margins surrounding the lobules

Table 2 The histological features (H) of 21 patients with basal cell carcinoma (BCC) on formalin-fixed, paraffin-embedded tissues according to BCC subtype compared with high-definition optical coherence tomography (HD) features

	Nodular BCC		Infundibulocystic BCC		Superficial BCC		Infiltrative BCC	
Features	H	HD	H	HD	H	HD	H	HD
Variable architectural disarray of epidermis								
Parakeratosis	+	+	+	+	+	+	+	+
Keratinocytic nuclear pleomorphism	+	+	+	+	+	+	+	+
Islands of basaloid cells (dark lobular structures causing structural disarray)								
Elongated monomorphic nuclei	+	+	+	+	+	+	+	+
Scant poorly demarcated cytoplasm	+	+	+	+	+	+	+	+
Polarization of elongated nuclei along same axis of orientation								
Streaming (polarization of nuclei in aggregate of tumour cells)	+	+	+	− or +	+	+	+	+
Palisading of the basaloid cells at the periphery of the islands	++	NP	+	NP	++	NP	− or +	NP
Lobulated islands or trabeculae surrounded by a less-reflective border	NP	++	NP	+	NP	++	NP	+
Islands of tumour cells surrounded by mucinous stroma	++	NP	+	NP	++	NP	− or +	NP
Separation of the tumour cells from the surrounding stroma (clefting)	++	NP	+	NP	++	NP	− or +	NP
Variable changes inside cell aggregations								
Mitotic figures	+	NP	+	NP	+	NP	+	NP
Apoptotic cells	+	+	+	+	+	+	+	+
Cystic changes (may resemble hair follicle)	− or +	− or +	++	++ (face)	−	−	−	−
Mucin production	− or +	− or +	− or +	− or +	− or +	− or +	− or +	− or +
Focal accumulation of melanin	− or +	−	−	−	−	−	−	−
Presence of dendritic cells	− or +	−	−	−	− or +	−	−	−
Within cell aggregations brightly reflective cells and structures	NP	+	NP	+	NP	− or +	NP	− or +
Large cell aggregations (*en face* imaging > 400 μm in diameter)	+	+	−	−	+	+	+	+
Small cell aggregations (*en face* imaging < 400 μm in diameter)	+	+	+	+	+	+	+	+
Islands in contact with epidermis (intermittently)	−	−	−	−	++	++	−	−
Elongated islands and cords (separated spatially, often angulated)	−	−	−	−	−	−	++	++
Variably reflective stroma	NP	++	NP	− or +	NP	+	NP	+
Prominent inflammatory infiltrate	++	++	− or +	− or +	++	+	− or +	− or +
Increased vascularity (*en face* image)	ND	++	ND	+	ND	++	ND	+
Dilated blood vessels (slice image)	++	++	−	+	++	++	+	+
Solar elastosis	+	+	+	− or +	+	+	+	+
Highly reflective margins surrounding the lobules (fibrous stroma)	NP	+	NP	− or +	NP	+	NP	++
Distortion (streaming effect) of collagen network	NP	++	NP	+	NP	++	NP	++
Deep part (> 750 μm) over the tumour	++	NP	++	NP	++	NP	++	NP
En face imaging	ND	++	ND	++	ND	++	ND	++

++, very strong; +, present; − or +, not always present; −, absent; NP, not possible; ND, not done routinely.

associated with distortion of the collagen network could not be demonstrated with standard microscopy. Features detected by standard microscopy of H&E-stained sections but not detected by HD-OCT included clefting and palisading of BCC cells and the deep part of the tumour over 570 μm.

Relevant HD-OCT features of BCC may be subdivided in to two groups according to the respective directions (Table 3). Relevant features in the axial direction are lobulated islands or trabeculae surrounded by a less-reflective border causing abnormal skin architecture. Deeper in the papillary dermis and upper reticular dermis highly reflective margins are surrounding the lobules corresponding with fibrous stroma. Solar elastosis is present as well as dilated blood vessels. Relevant features in the lateral direction are pleomorphism of the over-

Table 3 Features of basal cell carcinoma by reflectance confocal microscopy (RCM) and by multibeam optical coherence tomography (MB-OCT) implemented on high-definition optical coherence tomography (HD-OCT) images

Features	RCM	HD-OCT	MB-OCT
En face (lateral direction)			
Pleomorphism of the overlying epidermis indicative of actinic damage	+	+	–
Dark lobular structure causing abnormal architecture	+	+	–
Presence of elongated monomorphic basaloid nuclei	+	+	–
Polarization of these nuclei along the same axis of orientation	+	+	–
Prominent inflammatory infiltrate	+	+	–
Increased vasculature	+	+	–
Cross-sectional (axial direction)			
Dark lobular structure causing abnormal architecture	–	+	+
At the periphery of the lobules decreased reflectance appearing darker than the bulk of the lobules	–	+	+
Highly reflective margins surrounding the lobules corresponding with fibrous stroma	–	+	+
Dilated blood vessels	–	+	+

lying epidermis indicative of actinic damage and presence of elongated monomorphic basaloid nuclei polarized along the same axis of orientation. Highly reflective margins surrounding the lobules associated with a distortion of the collagen network appear to be a unique feature. There is also a prominent inflammatory cell infiltrate with increased vascularity.

HD-OCT may not only facilitate the *in vivo* diagnosis of BCC (Table 3), but may also aid in distinguishing BCC subtypes as relevant for therapeutic choices, e.g. surgery vs. nonsurgical treatment (Table 4). Typical HD-OCT features of infundibulocystic BCC are cystic changes of small aggregations suggesting follicle derivation and minimal stromal reaction. Superficial BCC is characterized in HD-OCT by small discrete dark lobular structures presenting intermittently along the basal layer. The less-reflective border surrounding these lobular structures, the stromal reaction and abnormal architecture (streaming effect) caused by these lobular structures are prominent. Elongated islands and cords separated spatially, often angulated and oriented almost perpendicular to the surface together with highly reflective margins surrounding these islands and cords are prominent HD-OCT features of infiltrative BCC. MB-OCT studies have demonstrated that it is not easy to differentiate between actinic keratosis lesions and BCC lesions.[9] Because of its cellular resolution HD-OCT might be able to differentiate between actinic keratosis lesions and BCC lesions. Further studies need to be undertaken to evaluate this.

Table 4 Features analysed by high-definition optical coherence tomography in 21 patients according to different subtypes of basal cell carcinoma (BCC)

Features	Nodular BCC	Infundibulocystic BCC	Superficial BCC	Infiltrative BCC
Variable architectural disarray of epidermis	+	+	+	+
Islands of basaloid cells (dark lobular structures causing abnormal architecture)	+	+	+	+
Polarization of elongated nuclei along same axis of orientation	+	– or +	+	+
Lobulated islands or trabeculae surrounded by a less-reflective border	++	+	++	+
Variable changes inside cell aggregations				
Cystic changes (may resemble hair follicle)	– or +	++	–	–
Lobulated islands or trabeculae surrounded by a less-reflective border	++	+	++	+
Large cell aggregations (*en face* imaging > 400 μm in diameter)	+	–	+	+
Small cell aggregations (*en face* imaging < 400 μm in diameter)	+	++	++	++
Islands in contact with epidermis (intermittently)	–	–	++	–
Elongated islands and cords (separated spatially, often angulated)	–	–	–	++
Variably refractile stroma	++	– or +	+	+
Prominent inflammatory infiltrate	++	– or +	+	– or +
Increased vascularity	++	+	++	+
Highly reflective margins surrounding the lobules corresponding with fibrous stroma	+	– or +	+	++
Distortion (streaming effect) of collagen network	++	+	++	++

++, very strong; +, present; – or +, not always present; –, absent.

The gold standard for diagnosis on a morphological level is still conventional excisional biopsy with subsequent histology. It may, however, be speculated that HD-OCT may serve as an important adjunct which may reduce the need for invasive biopsies in some of the cases, e.g. multiple tumours. Similarly, patients may request nonsurgical therapy, and in such cases HD-OCT makes it possible to conduct longitudinal studies of lesional therapy such as photodynamic therapy or other nonsurgical treatment procedures.

In conclusion, these results demonstrate that the relevant features previously defined for RCM and conventional OCT for detecting BCC can be implemented on the HD-OCT images. Secondly, relevant HD-OCT features for the *in vivo* diagnosis of BCC and for the differentiation of BCC subtypes compared with histology are suggested. Additional studies to test the sensitivity and specificity of the proposed criteria are essential to validate the findings of this pilot study.

What's already known about this topic?

- Reflectance confocal microscopy and conventional optical coherence tomography have proved successful in facilitating diagnosis of basal cell carcinoma (BCC).

What does this study add?

- High-definition optical coherence tomography may not only facilitate the *in vivo* diagnosis of BCC, but may also aid in distinguishing BCC subtypes as relevant for therapeutic choices.

References

1 Roewert-Huber J, Lange-Asschenfeldt B, Stockfleth E, Kerl H. Epidemiology and aetiology of basal cell carcinoma. *Br J Dermatol* 2007; **157** (Suppl. 2):47–51.

2 Flohil S, de Vries E, Neumann M *et al.* Incidence, prevalence and future trends of primary basal cell carcinoma in the Netherlands. *Acta Derm Venereol* (Stockh) 2011; **91**:24–30.

3 Sellheyer K. Basal cell carcinoma: cell of origin, cancer stem cell hypothesis and stem cell markers. *Br J Dermatol* 2011; **164**:696–711.

4 Carsin A, Sharp L, Comber H. Geographical, urban/rural and socioeconomic variations in nonmelanoma skin cancer incidence: a population-based study in Ireland. *Br J Dermatol* 2011; **164**:822–9.

5 Arits A, Schlangen M, Nelemans P, Kelleners-Smeets N. Trends in the incidence of basal cell carcinoma by histopathological subtype. *J Eur Acad Dermatol Venereol* 2011; **25**:565–9.

6 Olmedo J, Warschaw K, Schmitt J, Swanson D. Optical coherence tomography for the characterization of basal cell carcinoma *in vivo*: a pilot study. *J Am Acad Dermatol* 2006; **55**:408–12.

7 Gambichler T, Orlikov A, Vasa R *et al.* *In vivo* optical coherence tomography of basal cell carcinoma. *J Dermatol Sci* 2007; **45**:167–73.

8 Mogensen M, Jemec G. Diagnosis of nonmelanoma skin cancer/keratinocyte carcinoma: a review of diagnostic accuracy of nonmelanoma skin cancer diagnostic tests and technologies. *Dermatol Surg* 2007; **33**:421–5.

9 Mogensen M, Nürnberg B, Forman J *et al.* *In vivo* thickness measurement of basal cell carcinoma and actinic keratosis with optical coherence tomography and 20-MHz ultrasound. *Br J Dermatol* 2009; **160**:1026–33.

10 Mogensen M, Joergensen T, Nürnberg B *et al.* Assessment of optical coherence tomography imaging in the diagnosis of non-melanoma skin cancer and benign lesions versus normal skin: observer-blinded evaluation by dermatologists and pathologists. *Dermatol Surg* 2009; **35**:965–72.

11 Pomerantz R, Zell D, McKenzie G, Siegel D. Optical coherence tomography used as a modality to delineate basal cell carcinoma prior to Mohs micrographic surgery. *Case Rep Dermatol* 2011; **3**:212–18.

12 Gonzalez S, Tannous Z. Real-time, *in vivo* confocal reflectance microscopy of basal cell carcinoma. *J Am Acad Dermatol* 2002; **47**:869–74.

13 Nori S, Rius-Diaz F, Cuevas J *et al.* Sensitivity and specificity of reflectance-mode confocal microscopy for *in vivo* diagnosis of basal cell carcinoma: a multicenter study. *J Am Acad Dermatol* 2004; **51**:923–30.

14 Agero A, Busam K, Benvenuto-Andrade C *et al.* Reflectance confocal microscopy of pigmented basal cell carcinoma. *J Am Acad Dermatol* 2006; **54**:638–43.

15 Boone M. Optical coherence tomography: improved lateral and axial resolution: application in inflammatory skin diseases with epidermal alteration. 20th EADV Congress, Lisbon, Portugal, 20–24 October 2011; ePoster PO173.

16 Weedon D. *Weedon's Skin Pathology*, 3rd edn. Philadelphia: Elsevier Churchill Livingstone, 2009; 682–91.

17 Cockerell CJ, Tran KT, Carucci J *et al.* Basal cell carcinoma. In: *Cancer of the Skin* (Rigel DS, Robinson JK, Ross M, Friedman RJ, Cockerell CJ, Lim HW *et al.*, eds), 2nd edn. St Louis: Elsevier Saunders, 2011; 99–123.